

<sup>55</sup>J. Bardeen and R. Schrieffer, in *Progress in Low Temperature Physics*, edited by C. J. Gorter (North-Holland, Amsterdam, 1967), Vol. 3, p. 170.

<sup>56</sup>J. C. Swihart and W. Shaw (unpublished).

<sup>57</sup>A. B. Pippard, Proc. Roy. Soc. (London) **A216**, 547 (1963).

<sup>58</sup>R. G. Chambers, Proc. Roy. Soc. (London) **A215**, 481 (1952).

<sup>59</sup>J. Millstein and M. Tinkham, Phys. Rev. **158**, 3. (1967).

<sup>60</sup>V. L. Newhouse, *Applied Superconductivity* (Wiley, New York, 1964), p. 108.

<sup>61</sup>E. Erbach, R. L. Garwin, and M. P. Sarachik, IBM J. Res. Develop. **4**, 107 (1960); M. P. Sarachik, R. L. Garwin, and E. Erbach, Phys. Rev. Letters **4**, 52

(1960).

<sup>62</sup>P. B. Miller, Phys. Rev. **113**, 1209 (1959).

<sup>63</sup>M. D. Fiske, Rev. Mod. Phys. **36**, 221 (1964).

<sup>64</sup>The claim here is not that the total field within the film is symmetrically distributed, but that the field increment added to change the number of fluxoids from  $n$  to  $(n+1)$  is. The total current, including the bias current, is undoubtedly not zero at the center of the film. But this experiment measures the change in current as each fluxoid is added to the loop and this induced current is zero at the center of the film.

<sup>65</sup>A. M. Toxen, Phys. Rev. **123**, 442 (1963).

<sup>66</sup>B. W. Friday and J. L. Mundy, J. Appl. Phys. **40**, 2162 (1969).

## Thermal Conductivity of Superconducting Lead-Indium Alloys<sup>\*†</sup>

A. K. Gupta and S. Wolf

*Department of Physics, Case Western Reserve University, Cleveland, Ohio 44106*

(Received 7 February 1972)

The thermal conductivity in the mixed state  $K_m$  of a series of lead-indium alloys containing from 3 to 21 at. % In was measured as a function of temperature and magnetic field. The temperature dependence of the thermal conductivities in the superconducting and normal states  $K_s$  and  $K_n$ , respectively, was also measured in the range from 1.35 to 7.5 K. In the mixed state, the main emphasis was on the region near the upper critical field  $H_{c2}$  where Caroli and Cyrot found theoretically that the electronic thermal conductivity of dirty type-II superconductors varies linearly with applied magnetic field. In order to compare with their theory it was necessary to separate the electronic and lattice thermal conductivities, and to analyze the lattice contribution in terms of the scattering by boundaries, point defects, and conduction electrons. The field dependence of the lattice thermal conductivity was then theoretically calculated and subtracted from the experimentally measured field dependence of the total thermal conductivity. The experimental results are in good agreement in the dirty limit but large deviations are observed as the indium concentration is reduced. The phonon mean free path due to scattering by point defects was found to be in reasonably good agreement with the Klemens theory. The upper critical fields  $H_{c2}$  obtained from  $K$ -vs- $H$  curves were compared with the theory of Helfand and Werthamer. From the critical fields, the product of the electronic mean free path and the residual electrical resistivity was found to be  $0.66 \times 10^{-11} \Omega \text{ cm}^2$ . The coherence length in the pure limit  $\xi_0$  was also computed from the data and a value of 1060 Å was found.

### I. INTRODUCTION

The thermal conductivity of type-II superconducting alloys as a function of magnetic field, under certain circumstances, is observed to go through a minimum. Minima in the variation of thermal conductivity with magnetic field can also occur when an intermediate-state structure exists, and since early measurements<sup>1-4</sup> focused on the intermediate state the distinctive behavior of type-II superconductors was not at first recognized. Sladek<sup>5</sup> was the first to observe a minimum for In-Tl alloys even in the absence of the intermediate state. This work went unnoticed until Dubeck *et al.*<sup>6</sup> observed similar behavior for In-Bi alloys. They explained this behavior by considering the variation of the

spatially averaged energy gap with field and the dependence of the thermal conductivity on the energy gap as calculated by Bardeen, Rickayzen, and Tewordt (BRT).<sup>7</sup> They showed that the phonon conductivity should rapidly decrease as the magnetic field is increased beyond the lower critical field  $H_{c1}$ . For higher values of the field the phonon conductivity should decrease slowly and should reach the normal-state value at  $H = H_{c2}$ . At the same time the electronic thermal conductivity increases towards its value in the normal state as the field increases from  $H_{c1}$  to  $H_{c2}$ . The combination of the two effects yields the observed behavior. The depth of the minimum depends on the ratio of the thermal conductivity in the superconducting state to the normal state. When the conductivity

does not change very much in going from one phase to another the minimum may be very shallow or even absent.

Although the average-energy-gap model of Dubeck *et al.* was able to provide a good account of the general shape of the thermal-conductivity-vs-field curve, it was unsuccessful in following the experimental curve closely. Especially in the high-field region, Caroli and Cyrot<sup>8</sup> pointed out that the use of an average energy gap was inappropriate near the upper critical field, since, in fact, there was no energy gap in that region. They, in fact, predicted a linear variation of the electronic thermal conductivity with field, in agreement with the experiments but in contrast to the average-gap analysis. They also showed that the ratio at  $H_{c2}$  of the slope of the curve of the electronic thermal conductivity versus field to the slope of the magnetization curve was a universal function of the reduced temperature.

Del Vecchio and Lindenfeld<sup>9</sup> measured the thermal conductivity of In-Bi alloys and by using the theoretical values<sup>10</sup> for the slope of the magnetization compared their results with the Caroli-Cyrot theory. They found good agreement with the theory above a reduced temperature of 0.4 K, but below that temperature the experimental values were lower than the theoretical ones by up to 30%. They accounted for the discrepancy by suggesting a more rapid variation with temperature of  $\kappa_2$  than was theoretically predicted. Similar measurements on Nb alloys were made by Lowell and Sousa.<sup>11</sup> They found reasonable agreement with the theory for the most impure sample; for the other cases the experimental slopes considerably exceeded the theoretical value. Unfortunately, for their dirtiest sample, they did not report any measurements below a reduced temperature of 0.35.

Lindenfeld, Lynton, and Soulen<sup>12</sup> compared their thermal-conductivity data on two Pb-Bi alloys (strong-coupling type-II superconductors) with the Caroli-Cyrot theory. They did not separate out the contribution of the lattice conductivity, and therefore could only conclude that the agreement was worse for the purer sample. The present measurements were therefore undertaken to test the agreement between theory and experiment for strong-coupling type-II superconductors. In this work we have used the experimental values of magnetization and have made the appropriate separation of the lattice contribution to the thermal conductivity so as to eliminate any of the doubts remaining from previous experiments.

## II. EXPERIMENTAL DETAILS

The Pb-In alloy was prepared from 99.9999%-pure Pb (Cominco) and 99.999%-pure In (Indium Corp. of America). The alloy was made by melt-

ing the appropriate amounts of Pb and In in an evacuated Pyrex tube and vibrating the melt for more than 1 h. The melt was then quenched in cold water. The slugs so formed were etched in a solution of 80% acetic acid and 20% hydrogen peroxide (by volume). These were then extruded in a stainless-steel extruder to rods of  $\frac{1}{8}$  in. diam. These rods were cut into 3-cm lengths and were again etched with the acetic acid and hydrogen peroxide solution. The residual resistivity for different sections of the extruded wire was found to be the same within experimental error. This demonstrated the homogeneity of the sample. All the samples were annealed at 275 °C for at least a week in helium-filled Pyrex tubes.

The details of the experimental setup and measuring techniques are described elsewhere.<sup>13</sup> A brief description of the essential features is given here. The conventional steady-state method was used to measure the thermal conductivity. The sample inside a vacuum calorimeter was clamped at the end of a copper rod which was in contact with the outside liquid-helium bath through a heat station and a brass rod. Two heaters of No. 40 manganin wire were wound noninductively, one at the free end of the sample ( $H_1$ ) and the other ( $H_2$ ) on the brass rod. The heater  $H_2$  was used to raise the temperature of the sample above the helium-bath temperature and also to make the sample normal after each field cycle to eliminate the trapped flux. The sample heater was used to establish a thermal gradient along the sample for the thermal-conductivity measurements. The leads from the heat station to the sample were No. 40 manganin wires with the exception of the two leads carrying the heater ( $H_1$ ) current, which were 0.003-in.-diam Nb-25-at.-%-Zr wires chosen because no heat is developed in them below their superconducting transition temperature. The lengths of the leads connecting the sample to the heat station were chosen so that less than 0.1% of the heat developed in the heater ( $H_1$ ) traveled down the leads.

The temperature difference along the sample was measured by  $\frac{1}{10}$ -W Allen-Bradley carbon resistors. Over the temperature range 1.2–3 K, 56- $\Omega$  resistors were used while 330- $\Omega$  resistors were used over the temperature range 3–8 K. The carbon resistors were glued with GE 7031 varnish into holes in a small copper block having a knife edge at one end. These copper blocks were clipped onto the sample. A dc bridge was used to measure the resistances of the carbon thermometers. The circuit was designed to measure  $\Delta R$  directly so that any fluctuation in bath temperature influenced both the resistors equally and  $\Delta R$  was unaffected. All the carbon thermometers were calibrated against a calibrated germanium thermometer during each run. The temperatures were obtained by fit-

ting the resistances of the carbon thermometers at the calibration points to a modified Clement-Quinnell equation<sup>14</sup> of the form

$$\frac{1}{T^*} = A \ln R + \frac{B}{\ln R + D} + C.$$

The computer program for this fit started with a value for  $D$  and then least-squares fitted  $A$ ,  $B$ , and  $C$ . If the fit was not within some prescribed deviation,  $D$  was stepped and the process repeated. The final fit was quite good since  $T_{\text{calc}} - T^*$  was typically less than 1 mdeg and  $\Delta T^* = T_1^* - T_2^*$  was less than 0.1 mdeg for the calibration points. These constants ( $A$ ,  $B$ ,  $C$ , and  $D$ ) were then used to calculate the values of temperatures from the measured values of resistances.

The thermal conductivity was calculated by using the following expression:

$$K(\bar{T}) = \left( \frac{\dot{Q}}{T_1 - T_2} \right) \frac{L}{A},$$

where  $\bar{T} = \frac{1}{2}(T_1 + T_2)$ ,  $\dot{Q}$  is the power developed in the main heater which travels down the sample and is known to better than 0.1%,  $T_1 - T_2$  is the temperature difference between the thermometers and is known to better than 0.2%,  $L$  is the distance between the thermometers, and  $A$  is the cross-sectional area of the sample.  $L/A$  was known to better than 2%. This is the largest source of error in the thermal conductivity.

The measurements in the normal and mixed states were made by applying a longitudinal magnetic field.

### III. RESULTS

For each sample the thermal conductivity was measured as a function of temperature in the superconducting state (without magnetic field) and in the normal state in a sufficiently large magnetic field. The results for samples 1, 2, 3, and 4 which contained 3, 5, 10, and 21 at. % In, respectively, are shown in Fig. 1. The thermal conductivity  $K_m$  in the mixed state was also measured as a function of longitudinal magnetic field at selected temperatures. Figure 2 shows a representative curve of  $K$  vs  $H$  for Pb-3-at. % In alloy. The thermal conductivity remains constant up to the lower critical field  $H_{c1}$ , then it drops abruptly as the magnetic field is increased beyond  $H_{c1}$ , goes through a minimum, and then increases towards the normal-state value at  $H_{c2}$ . When the field is decreased, the same curve is followed until close to  $H_{c1}$  where it breaks away, rising to a lower value than the initial one, reflecting the known hysteretic behavior of type-II materials.

$K$ -vs- $H$  curves were plotted for each sample at different temperatures and  $(dK/dH)_{H=H_{c2}}$  was determined. Figures 3 and 4 show the values of  $(dK/dH)_{H=H_{c2}}$  obtained in this way, plotted against the reduced temperature  $t$ .

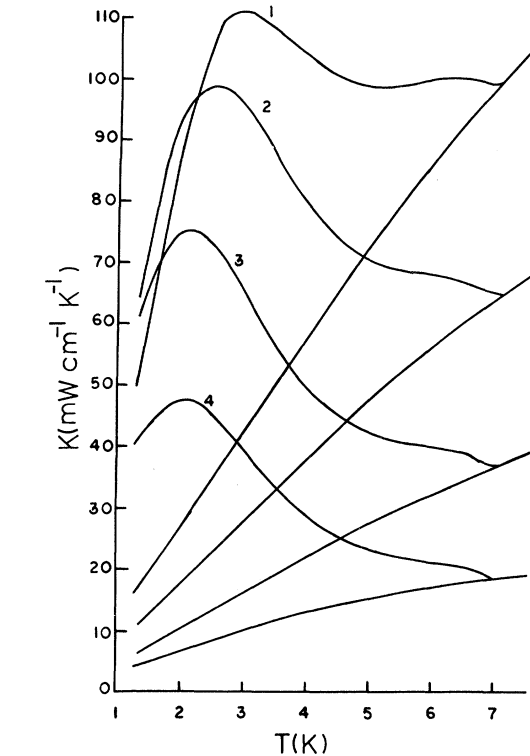


FIG. 1. Thermal conductivity vs temperature for samples 1, 2, 3, and 4. In each case the upper curve represents the results in the superconducting state and the lower curve represents the results in the normal state.

$(dH)_{H=H_{c2}}$  obtained in this way, plotted against the reduced temperature  $t$ .

The residual resistance of the samples was also measured using the standard four-terminal method. The resistivity at 4.2 K was obtained by applying magnetic fields greater than  $H_{c3}$  to quench completely superconductivity in each case. Table I lists the values of residual resistivity for all the four samples.

#### A. Determination of Parameters

Since  $K$ -vs- $H$  curves are reversible near  $H_{c2}$ , these measurements can be used for a more consistent determination of  $H_{c2}$  than the magnetization measurements which are irreversible. Figure 5 shows  $H_{c2}$  as a function of reduced temperature for all four samples. Helfand and Werthamer<sup>15</sup> calculated the temperature dependence of  $h^* = H_{c2}(t) / [-dH_{c2}(t)/dt]_{t=1}$  in the pure and dirty limits. Figure 6 shows the experimental results for our lowest- and highest-In-concentration alloys. The data for intermediate-concentration alloys lie in between the two results. For comparison, the theoretical curve of Helfand and Werthamer is also

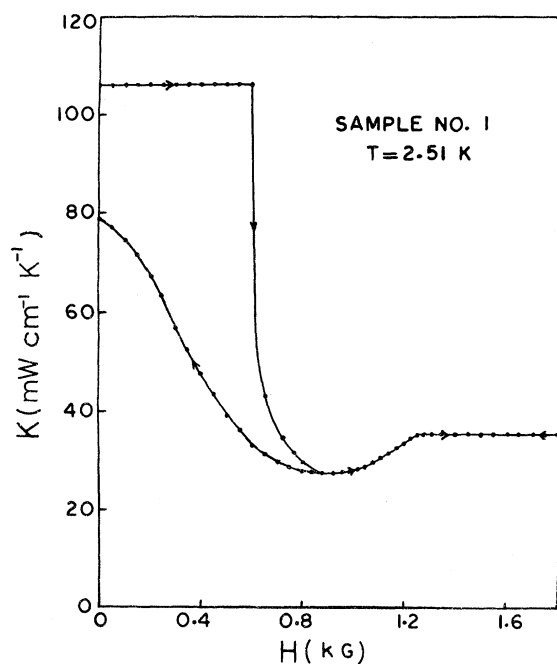


FIG. 2. Thermal conductivity vs applied magnetic field for sample No. 1 at 2.51 K.

drawn. We note that the results for the 3-at. %-In alloy are close to the pure-limit curve and the results for the 21-at. %-In alloy are close to the dirty limit. A previous determination of  $h^*$  from the magnetization measurements by Farrell, Chandrasekhar, and Culbert<sup>16</sup> showed that the experimental values for a single low-concentration alloy were lower than the theoretical dirty-limit curve. Our results do not show any such deviation from the theory.

The ratio  $\xi_0/l$  was calculated indirectly from Gor'kov's<sup>17</sup> relation

$$\kappa(l) = \kappa_0 / \chi(\Lambda),$$

where  $\kappa_0$  is the Ginzburg-Landau parameter in the pure limit,  $l$  is the average electronic mean free path, and

$$\chi(\Lambda) = \frac{8}{7\xi(3)} \sum_{n=0}^{\infty} \frac{1}{(2n+1)^2(2n+1+\Lambda)}.$$

Here  $\xi(3) = 1.202$  and  $\Lambda = 0.882 (\xi_0/l)$ . The value<sup>18</sup> of  $\kappa_0 = 0.24$  was used in these calculations. For  $\kappa(l)$ , the experimental values of Farrell, Chandrasekhar, and Culbert<sup>16</sup> were used. Since these authors did not measure a 3-at. % alloy, we plotted their values of  $\kappa$  as a function of In concentration and extrapolated to 3-at. % concentration. The calculated values of  $\xi_0/l$  for our samples are shown in Table I.

As a by-product of this work, it is now possible

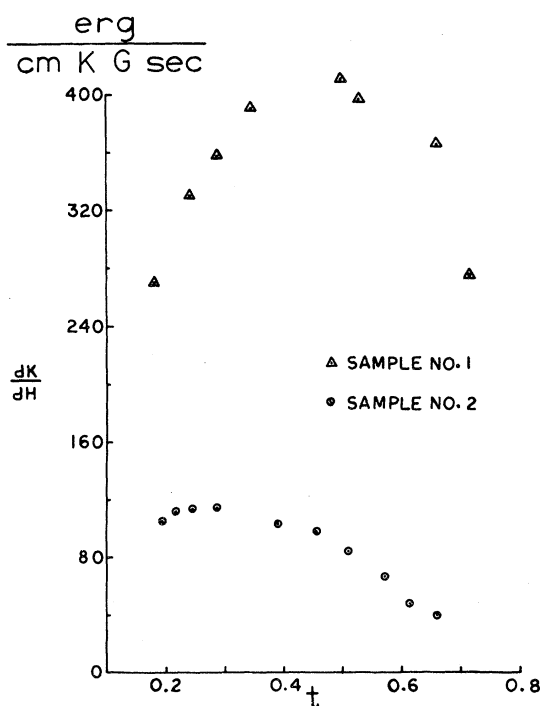


FIG. 3.  $(dK/dH)_{H=H_{c2}}$  vs reduced temperature for samples 1 and 2.

to determine  $\xi_0$ ,  $l$ , and hence  $\rho_0 l$ . We used the Gor'kov relation in the form used by Del Vecchio and Lindenfeld<sup>9</sup>:

$$\xi_0^2 = 0.605 \times 10^{-7} \frac{\kappa/\kappa_0}{T_c (-dH_{c2}/dT)_{T=T_c}}.$$

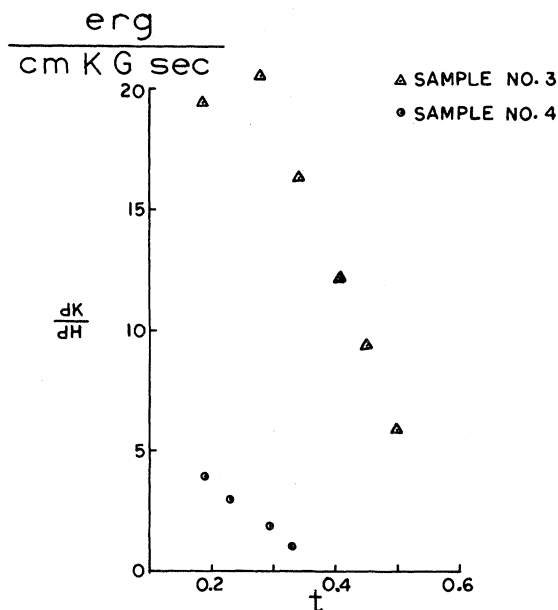


FIG. 4.  $(dK/dH)_{H=H_{c2}}$  vs reduced temperature for samples 3 and 4.

TABLE I. Characteristics and parameters of the alloys studied.

Parameter	Pb-3-at. %-In	Pb-5-at. %-In	Pb-10-at. %-In	Pb-21-at. %-In
$\rho_0$ ( $\mu\Omega$ cm)	2.08	3.64	6.68	12.20
$\kappa$	1.00	1.25	2.17	3.60
$T_c$ ( $^\circ$ K)	7.15	7.12	7.05	6.90
$\xi_0/l$	3.85	5.78	10.2	17.9
$l$ ( $\text{\AA}$ )	282	183	102	588
$\xi_0$ ( $\text{\AA}$ )	1088	1056	1042	1030
$\rho_0 l$ ( $10^{-11}$ $\Omega$ cm <sup>2</sup> )	0.59	0.66	0.68	0.70
$\left(-\frac{dH_{c2}}{dt}\right)_{t=1}$ (G)	2150	3100	5030	8580
$A$ (cm)	0.015	0.032	0.065	0.088
$B$ (cm <sup>-1</sup> deg <sup>-4</sup> )	0.12	0.23	0.53	1.28

The values of  $\xi_0$  are tabulated in Table I and centered about 1060  $\text{\AA}$ . The average value of  $\rho_0 l$  is  $0.66 \times 10^{-11}$   $\Omega$  cm<sup>2</sup>. The most recent values of  $\rho_0 l$  obtained by anomalous skin effect<sup>19</sup> and by cyclotron resonance<sup>20</sup> are  $1.06 \times 10^{-11}$  and  $0.9 \times 10^{-11}$   $\Omega$  cm<sup>2</sup>, respectively.

#### B. Lattice Thermal Conductivity

Thermal conduction in metals is due to contributions from the electrons ( $K_e$ ) and phonons ( $K_g$ ). Thus, the thermal conductivity in the normal metals is

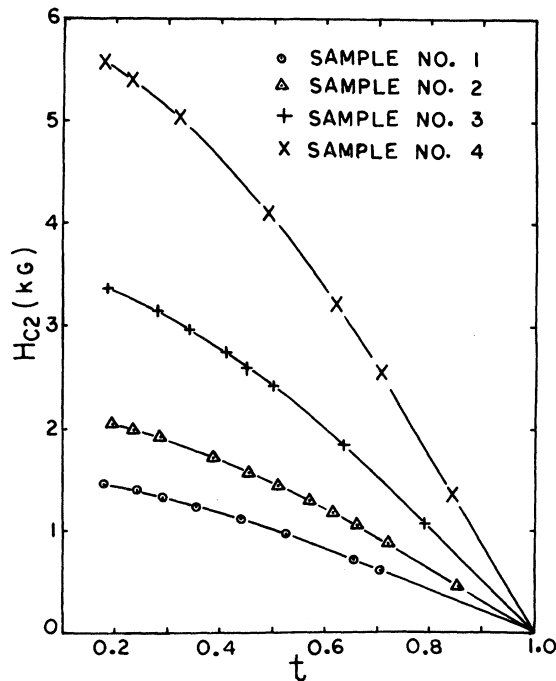
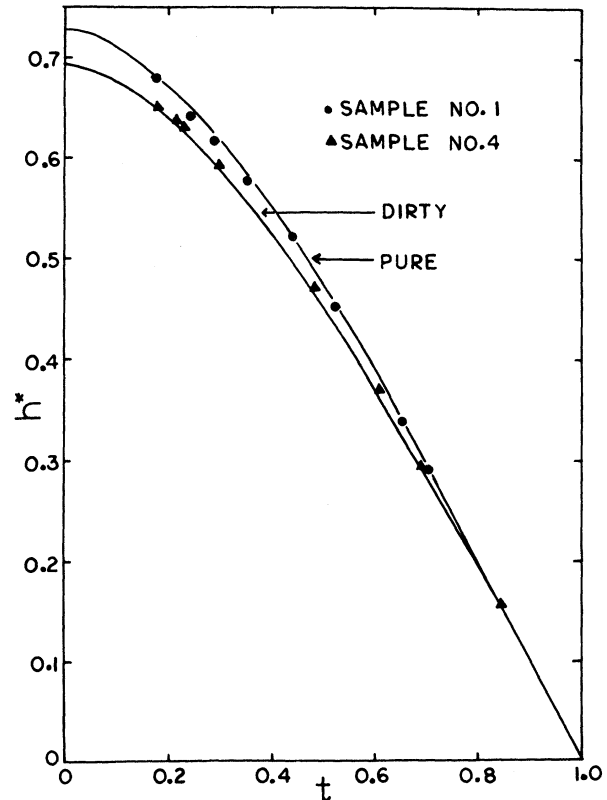


FIG. 5. Upper critical field vs reduced temperature.

$$K_n = K_{en} + K_{gn} .$$

Since our alloys contained at least 3 at. % In, the scattering of electrons by phonons was negligible in comparison to the scattering by impurities and therefore  $K_{en}$  was equal to  $L_0 T / \rho_0$  as given by the Wiedemann-Franz law (with  $L_0 = 2.445 \times 10^{-8}$  V<sup>2</sup>/deg<sup>2</sup>).

The phonon thermal conductivity may be described

FIG. 6.  $h^* \equiv H_{c2}(t) / (-dH_{c2}/dt)_{t=1}$  vs reduced temperature.

by the equation

$$K_g = \frac{k_B^4 T^3}{2\pi^2 \hbar^3 v_s^2} \int_0^\infty \frac{x^4 e^x dx}{(e^x - 1)^2 \sum(1/l_i)} \quad (1)$$

Here  $x = \hbar\omega/k_B T$  and  $v_s$  is the sound velocity;  $l_i$  are the phonon mean free paths due to individual scattering mechanisms. The scattering mechanisms which need to be considered for our samples are the boundaries, point defects, and the conduction electrons. Thus

$$k_{gn} = \frac{k_B^4 T^3}{2\pi^2 \hbar^3 v_s^2} \int_0^\infty \frac{x^4 e^x / (e^x - 1)^2 dx}{1/A + BT^4 x^4 + CTx} \quad (2)$$

Here  $A$  is the boundary mean free path.  $B$  and  $C$  are related to the phonon mean free paths due to the point defects and the conduction electrons, respectively. The phonon mean free path due to point defects was calculated by Klemens.<sup>21,22</sup> According to Klemens,

$$\frac{1}{l_{PD}} = \frac{3a^3 n \omega^4}{\pi v_s^4} S^2, \quad (3)$$

where  $a^3$  is the volume per atom,  $v_s$  is the velocity of sound, and  $n$  is the concentration of point defects. The scattering amplitude is

$$S^2 = S_1^2 + S_2^2, \quad (4)$$

where  $S_1$  is due to mass defects, i. e. ,

$$S_1^2 = \frac{1}{12} (\Delta M/M)^2. \quad (5)$$

$M$  is the average atomic mass and  $S_2$  is due to distortion and is given by<sup>23</sup>

$$S_2^2 = 3\gamma^2 (\Delta R/R)^2, \quad (6)$$

where  $\gamma$  is the Grüneisen constant and  $\Delta R/R$  is the fractional radial distortion of the lattice. Comparing Eqs. (2) and (3), we get

$$B = 3a^3 k_B^4 n / \pi v_s^4 \hbar^4. \quad (7)$$

In the superconducting state the BRT<sup>7</sup> theory with<sup>24</sup>  $2\epsilon_0 = 4.36kT_c$  was used to calculate  $K_{es}$ . (This procedure is invalid for pure strong-coupling superconductors such as lead. However, our alloys are sufficiently dirty and the scattering of electrons by phonons is negligible. Preliminary results on the measurement of electronic thermal conductivity of thin films of Pb-3-at. %In showed that  $K_{es}/K_{en}$  is given by the BRT relation with  $2\epsilon_0 \sim 4.36kT_c$ .) When electrons are scattered by impurities, BRT found that

$$R_e \equiv \frac{K_{es}}{K_{en}} = \frac{2F_1(-y) + 2y \ln(1 + e^{-y}) + y^2/(1 + e^y)}{2F_1(0)},$$

where

$$y = \epsilon(T)/k_B T$$

and

$$F_n(-y) = \int_0^\infty \frac{z^n dz}{1 + e^{z+y}}.$$

Here  $2\epsilon(T)$  is the temperature-dependent gap.

Thus,

$$K_{gs} = K_s - R_e L_0 T / \rho_0.$$

In  $K_{gs}$ , the contributions due to boundary and point defects will be the same as in the normal state.

The phonon mean free path  $l_e$  due to the scattering by electrons will be increased in the superconducting state, giving rise to an increase in lattice thermal conductivity. BRT<sup>7</sup> calculated the ratio  $l_{es}^{-1}/l_{en}^{-1} \equiv g(x)$  in zero field. Thus,  $K_{gs}$  is given by

$$K_{gs} = \frac{k_B^4 T^3}{2\pi^2 \hbar^3 v_s^2} \int_0^\infty \frac{x^4 e^x / (e^x - 1)^2 dx}{1/A + BT^4 x^2 + CTxg(x)}. \quad (8)$$

We separated out the lattice thermal conductivities  $K_{gn}$  and  $K_{gs}$  from the measured conductivities  $K_n$  and  $K_s$  for all four alloys. When  $K_{gn}/T$  vs  $T$  was plotted, the low-temperature points lay on a straight line indicating that the scattering of phonons by conduction electrons is dominant at these low temperatures. Thus the value of  $C$  in Eq. (2) was determined from the low-temperature data for  $K_{gn}$  and by assuming the first two terms in the denominator were zero. The integrals of Eqs. (2) and (8) were then performed for various values of  $A$  and  $B$  at a series of reduced temperatures. At each temperature the experimental curve could be fitted by different combinations of parameters. For each value of  $A$ , the value of  $B$  which best fitted the data was plotted and a line drawn through all these points. The intersection of the lines for various temperatures gave the values of  $A$  and  $B$  which best fitted the data at all temperatures. These values of  $A$  and  $B$  are given in Table I. A typical fit for Pb-10-at. %In alloy is shown in Fig. 7. The solid curve represents the data and the points are the results of the best fit.

The value of  $B$  can also be evaluated by Klemens's theory using Eq. (7). Table II lists the values of  $B$  for different alloys. The second column of Table II lists the values of  $B$  obtained by best fitting the data. The third column is the theoretical value of  $B$  when only the mass-defect term is considered. As can be seen, these computed values are less than or equal to half the experimental values. The fourth column gives the contributions due to the lattice-distortion term and the last column gives the sum of the two contributions. In the calculation of the lattice-distortion term the value of  $\gamma$  was taken to be equal to 2.73.<sup>25</sup> The fractional

TABLE II. Values of  $B$  for the alloys studied.

Sample No.	$B_{\text{expt.}}$ ( $\text{cm}^{-1} \text{deg}^{-4}$ )	$B_{\text{mt}}$ ( $\text{cm}^{-1} \text{deg}^{-4}$ )	$B_{\text{ld}}$ ( $\text{cm}^{-1} \text{deg}^{-4}$ )	$B_t$ ( $\text{cm}^{-1} \text{deg}^{-4}$ )
1	0.12	0.06	0.11	0.17
2	0.23	0.10	0.19	0.29
3	0.53	0.20	0.39	0.59
4	1.28	0.43	0.82	1.25

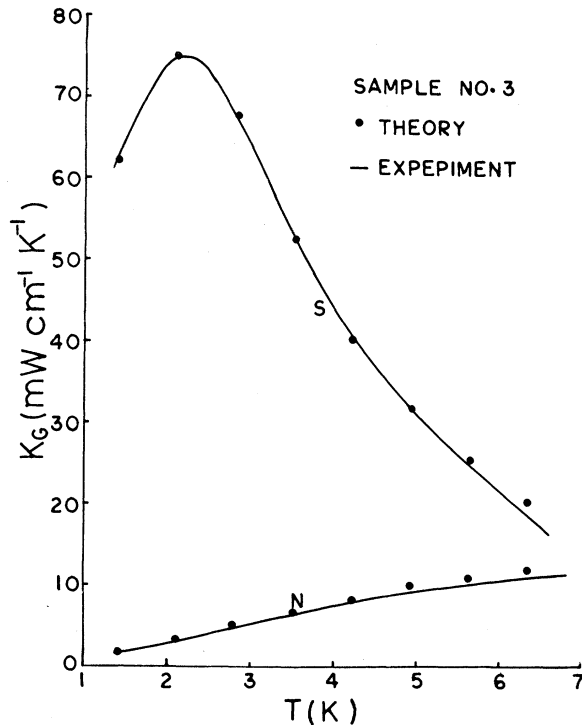


FIG. 7. Lattice thermal conductivity vs temperature for sample 3. Solid line represents the data and the points are the results of best fit. The upper curve represents the results in the superconducting state and the lower curve represents the results in the normal state.

radial distortion calculated from the observed change in the lattice spacings<sup>26</sup> of Pb-In alloys was equal to 0.048. The general method used to evaluate  $(\Delta R/R)$  was the same as used by Giedd and Reynolds.<sup>27,28</sup> It was assumed that the atoms were hard spheres closepacked in a cube of side 4.94 Å. Therefore the radius  $R$  of the sphere equals 1.746 Å. Since the value of the lattice constant was decreased by 0.017 Å when 10 at. % of indium was added, so  $\Delta R = 0.0085$  or  $\Delta R/R = 0.0048$  for 0.1 fraction of impurity. Thus the fractional radial distortion of the lattice was equal to 0.048.

We note that the theoretical value  $B_i$  is somewhat higher than the experimental value except for 21-at. %-In concentration. The theoretical values were calculated by assuming  $S^2 = S_1^2 + S_2^2$ . However, it is possible to calculate  $S^2$  from the relationship  $S^2 = (S_1 + S_2)^2$ , but since  $S_1$  and  $S_2$  have an unknown phase relation that makes it difficult to sum them together in this way. If they are calculated using the square roots of Eqs. (5) and (6), the resulting  $S^2$  gives a value of  $B$  much larger than that computed using  $S^2 = S_1^2 + S_2^2$ . This probably means that  $S_1$  and  $S_2$  are not in phase with each other, and it is better to square them first to remove the phase relationship before adding them together to form  $S^2$ .

### C. Comparison with Caroli-Cyrot Theory

Caroli and Cyrot<sup>8</sup> calculated the electronic thermal conductivity of dirty type-II superconductors, for fields close to the upper critical field  $H_{c2}$ . They showed that

$$\left( \frac{dK_e/dH}{4\pi dM/dH} \right)_{H=H_{c2}} = - \frac{c k_B}{2e} \left( 1 + \frac{\rho_c \psi^{(2)}(\frac{1}{2} + \rho_c)}{\psi^{(1)}(\frac{1}{2} + \rho_c)} \right),$$

where  $\psi^{(2)}$  is the tetragamma function and  $\psi^{(1)}$  is the trigamma function.  $\rho_c$  is given by the equation

$$\ln(T/T_c) = \psi(\frac{1}{2}) - \psi(\frac{1}{2} + \rho_c),$$

where  $\psi$  is the digamma function. Thus at  $H_{c2}$  the ratio  $[(dK_e/dH)/(4\pi dM/dH)]$  is a function of reduced temperature only.

In order to compare our thermal-conductivity results with the theory we used the experimental results of Farrell, Chandrasekhar, and Culbert<sup>16</sup> for  $(dM/dH)_{H=H_{c2}}$ . The field dependence of the lattice thermal conductivity was also calculated<sup>9</sup> by using Eq. (8) with parameters  $A$  and  $B$  found in Sec. III B and  $g(x, H) = [\alpha_T(H)/\alpha_T(H_{c2})]$  as calculated by Maki<sup>29</sup> where  $\alpha_T$  is the transverse ultrasonic attenuation coefficient. These values of  $K_g(H)$  were subtracted from the measured values of  $K(H)$  to get  $K_e(H)$ .  $K_e$  vs  $H$  was plotted and  $(dK_e/dH)_{H=H_{c2}}$  was determined. Figure 8 shows the final results for the

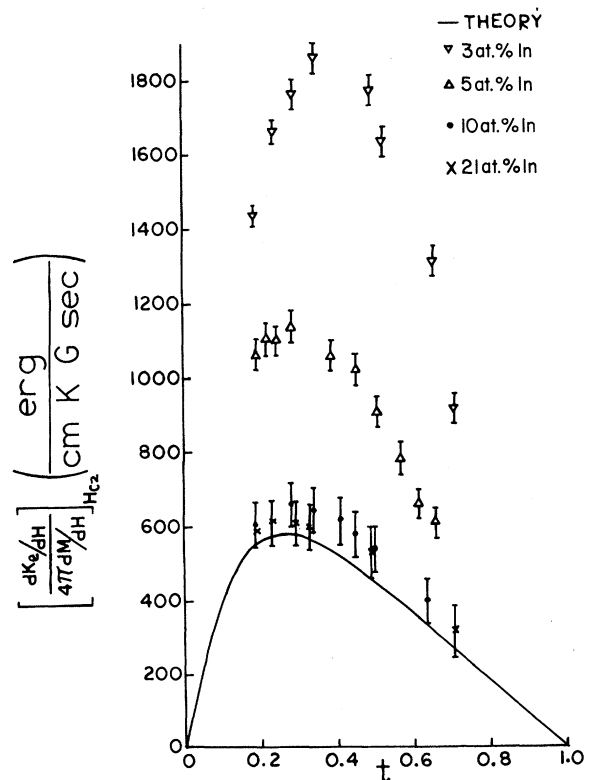


FIG. 8. Ratio  $[(dK_e/dH)/(4\pi dM/dH)]_{H=H_{c2}}$  as a function of reduced temperature.

ratio  $[(dK_e/dH)/(4\pi dM/dH)]_{H=H_{c2}}$  along with the universal curve of Caroli and Cyrot. The experimental results agree with the theory for samples 3 and 4. However, for samples 1 and 2 the slope is much larger than predicted by the theory.

We note from Table I that the value of  $\xi_0/l$  is 3.85 and 5.78 for samples 1 and 2, respectively, that is, these samples are not in the dirty limit. The values of  $\xi_0/l$  for samples 3 and 4 are close to the dirty limit; thus the experimental results agree with the theory in the dirty limit. The alloys in the intermediate-purity limit have a much larger value of the ratio  $[(dK_e/dH)/(4\pi dM/dH)]_{H=H_{c2}}$  than predicted by the theory and the disagreement increases with the decrease in impurity concentration. Similar behavior was noted by Lowell and Sousa<sup>11</sup> for TaNb alloys of intermediate purity and by Wasim and Zebouni<sup>30</sup> for niobium of intermediate purity.

#### IV. SUMMARY

The present study shows that the electronic thermal conductivity  $K_{em}$  in the mixed state of Pb-In alloys (strong-coupling superconductors) is in good agreement with the Caroli-Cyrot theory in the dirty limit. For the alloys in the intermediate limit there is qualitative agreement with the theory inasmuch as  $K_{em}$  increases linearly as  $H$  approaches  $H_{c2}$ ; but the ratio  $[(dK_{em}/dH)/(4\pi dM/dH)]_{H=H_{c2}}$  has

a higher value than predicted by the theory. This disagreement increases as the impurity concentration is reduced.

The lattice thermal conductivity at low temperatures of well-annealed alloys can be analyzed in terms of the scattering of phonons by the boundaries, point defects, and conduction electrons. The phonon mean free path due to point defects is in reasonably good agreement with the Klemens theory.

The upper critical fields  $H_{c2}$  obtained from  $K$ -vs- $H$  curves are in good agreement with the theory of Helfand and Werthamer.<sup>15</sup> Previous determination of  $H_{c2}$  from the magnetization measurements by Farrell, Chandrasekhar, and Culbert<sup>16</sup> showed some deviation from the theory for low-In-concentration alloys. Our results do not show any such deviations from the theory.

#### ACKNOWLEDGMENTS

We wish to thank Dr. B. S. Chandrasekhar for his advice and encouragement through all phases of this experiment. We would also like to thank Dr. L. V. Del Vecchio for the use of his program to calculate the field-dependent phonon contribution to the thermal conductivity. We have enjoyed many stimulating discussions with Dr. P. Lindenfeld and Dr. D. Farrell about many aspects of this work.

\*Research sponsored by the Air Force Office of Scientific Research, Office of Aerospace Research, United States Air Force, under AFOSR Contract No. F44620-69-C-0077.

†This paper is based on a thesis submitted by A. K. Gupta in partial fulfillment of the requirements for the Ph. D. degree at Case Western Reserve University, 1971.

<sup>1</sup>K. Mendelssohn and J. L. Olsen, Proc. Phys. Soc. (London) **A63**, 2 (1950).

<sup>2</sup>K. Mendelssohn and J. L. Olsen, Phys. Rev. **80**, 859 (1950).

<sup>3</sup>J. L. Olsen, Proc. Phys. Soc. (London) **A65**, 518 (1952).

<sup>4</sup>K. Mendelssohn and C. A. Schiffman, Proc. Roy. Soc. (London) **A255**, 199 (1960).

<sup>5</sup>R. J. Sladek, Phys. Rev. **97**, 902 (1955).

<sup>6</sup>L. Dubeck, P. Lindenfeld, E. A. Lynton, and H. Rorher, Phys. Rev. Letters **10**, 98 (1963).

<sup>7</sup>J. Bardeen, G. Rickayzen, and L. Tewordt, Phys. Rev. **113**, 982 (1959).

<sup>8</sup>C. Caroli and M. Cyrot, Physik Kondensierten Materie **4**, 285 (1965).

<sup>9</sup>L. V. Del Vecchio and P. Lindenfeld, Phys. Rev. B **1**, 1097 (1970).

<sup>10</sup>G. Eilenberger, Phys. Rev. **153**, 584 (1967).

<sup>11</sup>J. Lowell and J. B. Sousa, J. Low Temp. Phys. **3**, 65 (1970).

<sup>12</sup>P. Lindenfeld, E. A. Lynton, and R. Soulen, Proceedings of the Tenth International Conference on Low Temperature Physics, Moscow, 1966, Vol. 2, p. 396 (unpublished).

<sup>13</sup>A. K. Gupta, Ph. D. thesis (Case Western Reserve

University, 1971) (unpublished).

<sup>14</sup>J. F. Cochran, C. A. Schiffman, and J. P. Neighbor, Rev. Sci. Instr. **37**, 499 (1966).

<sup>15</sup>E. Helfand and N. R. Werthamer, Phys. Rev. Letters **13**, 686 (1964); Phys. Rev. **147**, 288 (1966).

<sup>16</sup>D. E. Farrell, B. S. Chandrasekhar, and H. V. Culbert, Phys. Rev. **177**, 694 (1969).

<sup>17</sup>L. P. Gor'kov, Zh. Eksperim. i Teor. Fiz. **37**, 1407 (1959) [Sov. Phys. JETP **10**, 998 (1960)].

<sup>18</sup>F. W. Smith, A. Bartoff, and M. Cardona, Physik Kondensierten Materie **12**, 145 (1970).

<sup>19</sup>R. G. Chambers, Proc. Roy. Soc. (London) **A215**, 481 (1952).

<sup>20</sup>J. E. Aubrey, Phil. Mag. **5**, 1001 (1960).

<sup>21</sup>P. G. Klemens, Proc. Phys. Soc. (London) **A68**, 1113 (1955).

<sup>22</sup>P. G. Klemens, Solid State Phys. **7**, 1 (1958).

<sup>23</sup>J. E. Gueths, P. L. Garbarino, M. A. Mitchell, P. G. Klemens, and C. A. Reynolds, Phys. Rev. **178**, 1009 (1969).

<sup>24</sup>J. G. Adler, J. E. Jackson, and T. A. Will, Phys. Letters **24A**, 407 (1967).

<sup>25</sup>M. J. Druyvesteyn, Philips Res. Rept. **1**, 77 (1946).

<sup>26</sup>C. Tyzack and G. V. Raynor, Acta Cryst. **7**, 505 (1954).

<sup>27</sup>R. E. Giedd and C. A. Reynolds, Phys. Rev. B **2**, 3533 (1970).

<sup>28</sup>R. E. Giedd (private communications).

<sup>29</sup>K. Maki, Phys. Rev. **158**, 397 (1967).

<sup>30</sup>S. M. Wasim and N. H. Zebouni, Phys. Rev. **187**, 539 (1969).